An alternative derivation of Katsevich's cone-beam reconstruction formula

Guang-Hong Chen[a)]
Department of Medical Physics, University of Wisconsin, Madison, Wisconsin 53792

(Received 26 December 2002; revised 2 October 2003; accepted for publication 2 October 2003; published 21 November 2003)

In this paper an alternative derivation of Katsevich's cone-beam image reconstruction algorithm is presented. The starting point is the classical Tuy's inversion formula. After (i) using the hidden symmetries of the intermediate functions, (ii) handling the redundant data by weighting them, (iii) changing the weighted average into an integral over the source trajectory parameter, and (iv) imposing an additional constraint on the weighting function, a filtered backprojection reconstruction formula from cone beam projections is derived. The following features are emphasized in the present paper: First, the nontangential condition in Tuy's original data sufficiency conditions has been relaxed. Second, a practical regularization scheme to handle the singularity is proposed. Third, the derivation in the cone beam case is in the same fashion as that in the fan-beam case. Our final cone-beam reconstruction formula is the same as the one discovered by Katsevich in his most recent paper. However, the data sufficiency conditions and the regularization scheme of singularities are different. A detailed comparison between these two methods is presented. © *2003 American Association of Physicists in Medicine.* [DOI: 10.1118/1.1628413]

I. INTRODUCTION

Since the concepts of Radon space, the Radon transform, and the reconstruction via steps of filtering and backprojection (FBP) are very successful in two-dimensional pencil beam and fan beam projections, it is our wish to extend the above success into the problem of image reconstruction from cone beam projections. In particular, it is desired to preserve the FBP structure of fan beam reconstruction in the cone-beam reconstruction algorithms. With this obvious goal in mind, Feldkamp, Davis, and Kress (FDK)[1] proposed an algorithm to reconstruct images from cone beam projections with a circular source trajectory. When the cone angle is small (up to approximately 10°), FDK algorithm produces images with tolerable artifacts. For a general source trajectory, an FDK-like approximate reconstruction scheme was proposed in Ref. 2.

Exact image reconstruction schemes from cone beam projections have also been proposed. In the context of medical imaging, it seems that the first inversion formula was proposed by Tuy.[3] An important feature in Tuy's inversion scheme is that the concepts of radon space, the radon transform, and the inverse radon transform were not explicitly invoked. The other early inversion scheme was proposed by Smith.[4] An essential difference between Tuy's inversion scheme and Smith's inversion scheme is that different filtering functions were used.[5] However, due to the difficulties and complexities in numerical implementation,[6,7] both algorithms are not generally accepted in practice. But their data sufficiency conditions are widely appreciated in the discussion of the cone beam reconstruction.

In the later development, other cone-beam reconstruction schemes were also discovered. One such milestone was provided by Grangeat.[8] In his algorithm, Grangeat established an important identity between cone beam projections and the first-order derivative of the Radon transform in $\mathbb{R}^3$. This important relation allows us to reconstruct the image by directly employing the three-dimensional inverse Radon transform. At the same time, one should also notice that the FBP structure is lost in Grangeat's algorithm. To remedy this drawback, Defrise and Clack[9] and Kudo and Saito[10] improved Grangeat's algorithm to make it FBP-type by introducing a shift variant filtering kernel. To reduce the computational complexity, Axelsson and Danielsson[11] adapted the linogram method for the Grangeat method. This approach resulted in a computational complexity of $O(N^3 \log N)$. For a more complete review of the approximate and exact cone beam reconstruction methods, we refer the readers to Ref. 12.

Recently, Katsevich[13,14] presented some cone-beam reconstruction algorithms for the spiral CT. There are several nice features in his reconstruction formulas. First, these formulas are mathematically exact. Second, the FBP structure is preserved with a shift-invariant filtering kernel. Third, the long object problem is nicely solved with the above-mentioned shift-invariant FBP reconstruction formulas. In his most recent paper,[15] Katsevich proposed a general reconstruction scheme for a general source trajectory which can be made to preserve the FBP structure with a shift-invariant filtering kernel upon choosing an appropriate weighting function. He also proved that the aforementioned reconstruction formulas for the spiral trajectory are special cases of the general formula when it is applied to the spiral source trajectory.

In our previous paper,[16] we formulated a framework for the image reconstruction from fan beam projections. In this framework, the radon inversion formula was not used. Instead, we started with a Tuy-like inversion scheme. Weighting the redundant data and rewriting the weighted summation into an integral along the source trajectory resulted in a shift-invariant FBP reconstruction formula with the following data sufficiency condition. Any straight line passing through a region of interest (ROI) should intersect the source trajectory at least once. Since the inverse radon transform is

not explicitly used in the derivation, the disparity of the inverse radon transforms in the two dimensional and three dimensional cases do not appear. This implies that the same procedure can be used to derive a FBP reconstruction formula in the cone beam case.

In the present paper, we explore how to derive a FBP reconstruction algorithm from cone beam projections by using the same procedure as we did in the fan beam case. In other words, we discuss how to derive a FBP cone-beam reconstruction formula from the classical Tuy's inversion formula. The final results in this paper provide a positive answer to the question on Tuy's inversion formulation raised by Natterer in his famous book:[17] ''It is not clear if it (Tuy's formula) can be turned into an efficient reconstruction algorithm.'' It is interesting that the application of our framework in the cone-beam case results in the same reconstruction formula as the one derived by Katsevich in his most recent paper.[15] However, there are several differences in our derivation from the one used by Katsevich. First, the regularization schemes for potential singularities are different. We propose to regularize the singularity by a signum function $\mathrm{sgn}[\hat{k}\cdot\mathbf{y}'(t)]$. In contrast, Katsevich introduced an extra regulator to erase the singularities during the calculation and a limit was taken at the very end of the calculations. For convenience, we call our regularization scheme a ''sgn-regulator'' and Katsevich's regularization scheme an ''η-regulator.'' The η-regulator is an auxiliary cut-off function to erase the potential sigularities at $\hat{k}\cdot\mathbf{y}'=0$. It has been introduced at the beginning of the derivation. In our derivation, the singularities at $\hat{k}\cdot\mathbf{y}'=0$ have been excluded temporarily. After Eq. (27) is derived, the sgn-regulator is proposed to take care of the effects of sigularities. Logically, the sgn-regulator needs to be justified *a posteriori*. This logic is generally used in physics and engineering, but it does not satisfy the rigorous requirements in pure mathematics. In other words, our sgn-regulator is more heuristic but less rigorous than the η-regulator in terms of the requirements of pure mathematics. These two regularization schemes are complementary in understanding of cone-beam image reconstruction. The second difference lies in the fact that the data sufficiency conditions are slightly different. Our data sufficiency condition can be summarized as: *Any plane cutting through a ROI should intersect the source trajectory at least once in a non-ended way*. The ''nontangential'' condition in Tuy's original data sufficiency conditions is relaxed in the present paper. As we discussed in the fan-beam case,[16] after performing integration by parts, the nonended condition could be further relaxed. In contrast, Katsevich's data sufficiency conditions contain two additional mild conditions. Third, an explicit and necessary constraint on the normalized weighting function [see Eq. (46)] has been derived for the final reconstruction formula. Some other technical differences will be pointed out in the text. Besides the above-noted differences, we believe that it is an important endeavor to establish the links among different reconstruction schemes as emphasized by Defrise and Clack.[5]

The layout of the paper is the following: In Sec. II, we review Tuy's inversion scheme. This brief review has two motivations. First, conventions and mathematical notation used throughout this paper are introduced. Second, we elaborate on the data sufficiency condition. Readers who are familiar with Tuy's formulation may skip the mathematical steps in this section. However, readers are encouraged to pay attention to the discussion on the data sufficiency condition in the last part of this section. Section III is devoted to the relaxation of nontangential condition in Tuy's scheme and the derivation of a FBP reconstruction formula by imposing a constraint on the weighting functions. Conclusions and further discussions will be found in Sec. IV.

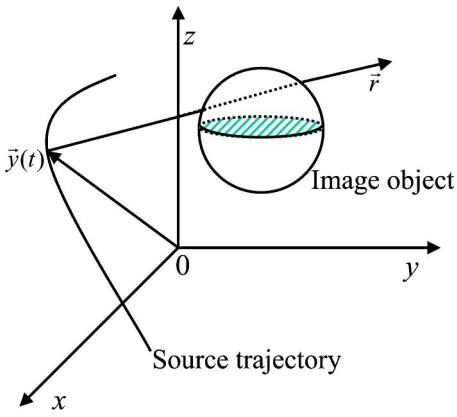

FIG. 1. The geometry used to define a cone-beam projection.

II. REVIEW OF TUY'S INVERSION FORMULA

In this section, we review Tuy's cone-beam reconstruction scheme. We define a cone-beam projection $g(\mathbf{r},\mathbf{y})$ by using a focal point vector $\mathbf{y}$ and a ray vector $\mathbf{r}$ (see Fig. 1) as follows:

$$g[\mathbf{r},\mathbf{y}(t)]=\int_0^\infty ds\, f[\mathbf{y}(t)+s\mathbf{r}], \tag{1}$$

where the focal point vector $\mathbf{y}(t)$ is parametrized by a single scalar parameter t. The image function $f(\mathbf{x})$ is assumed to have a compact support Ω. That is, the image function takes zero value outside the region Ω. Starting with the above-given definition, one can check the following scaling property for the cone-beam projections:

$$g(\mathbf{r},\mathbf{y})=\frac{1}{r}g(\hat{r},\mathbf{y}), \tag{2}$$

where a vector is decomposed into its magnitude and a unit vector which is denoted by a caret throughout the present paper, e.g., $\mathbf{r}=r\hat{r}$.

Although the translational invariance is lost in an individual view of divergent beam projections, we still want to connect the x-ray projections defined in Eq. (1) with the inverse Fourier transform of the image function $f(\mathbf{x})$ such that one can use the inverse Fourier transform to solve the image reconstruction problem. Thus, we introduce an intermediate function. In the cone-beam case, we follow Tuy[3] to

define an intermediate function $G_3(\mathbf{k},\mathbf{y})$ by taking a partial Fourier transform of Eq. (1) with respect to the vector $\mathbf{r}$. That is

$$G_3(\mathbf{k},\mathbf{y})=\int_{R^3} d^3\mathbf{r} g(\mathbf{r},\mathbf{y}) e^{-i2\pi\mathbf{k}\cdot\mathbf{r}}. \tag{3}$$

Using this definition and the scaling property (2), one can show that an important scaling property exists in $G_3(\mathbf{k},\mathbf{y})$, i.e.,

$$G_3(\mathbf{k},\mathbf{y})=\frac{1}{k^2}G_3(\hat{k},\mathbf{y}). \tag{4}$$

That is, $G_3(\mathbf{k},\mathbf{y})$ is a degree -2 homogeneous function. In contrast, the intermediate function $G_2[\hat{k},\mathbf{y}(t)]$ in the fan-beam case is degree -1 homogeneous function.[16] Our experience with the fan-beam case also suggests that we should have a way to represent $G_3[\mathbf{k},\mathbf{y}(t)]$ in terms of the fundamental degree -2 homogeneous functions $\delta'(x)$ and $1/x^2$ (or a regularized version of the ramp filter). We will come to this point again in Sec. III. After substituting Eq. (1) into Eq. (3) and changing the variables as follows:

$$\mathbf{z}=\mathbf{y}+s\mathbf{r}, \tag{5}$$

$$d^3\mathbf{r}=\frac{1}{s^3}d^3\mathbf{z}, \tag{6}$$

we obtain

$$\begin{aligned} G_3(\mathbf{k},\mathbf{y}) &= \int_0^\infty \frac{ds}{s^3} e^{i2\pi\mathbf{k}\cdot\mathbf{y}/s}\int d^3\mathbf{z} f(\mathbf{z}) e^{-i2\pi\mathbf{z}\cdot\mathbf{k}/s} \\ &= \int_0^\infty \frac{ds}{s^3} e^{i2\pi\mathbf{k}\cdot\mathbf{y}/s}\tilde{f}\left(\frac{\mathbf{k}}{s}\right). \end{aligned} \tag{7}$$

Here $\tilde{f}(\mathbf{k})$ is the Fourier transform of the image function $f(\mathbf{x})$. It is defined by

$$\tilde{f}(\mathbf{k})=\int_{R^3} d^3\mathbf{x} f(\mathbf{x}) e^{-i2\pi\mathbf{x}\cdot\mathbf{k}}. \tag{8}$$

To further simplify Eq. (7), we change variables again from s to τ through $\tau=k/s$. We thus obtain

$$\begin{aligned} G_3(\mathbf{k},\mathbf{y}) &= \int_0^\infty \frac{ds}{s^3}\tilde{f}\left(\frac{\mathbf{k}}{s}\right)e^{i2\pi\mathbf{k}\cdot\mathbf{y}/s} = \frac{1}{k^2}\int_0^\infty d\tau\tau\tilde{f}(\tau\hat{k})e^{i2\pi\tau\hat{k}\cdot\mathbf{y}} \\ &= \frac{1}{k^2}\int_0^\infty d\tau\tau\tilde{f}(\boldsymbol{\tau})e^{i2\pi\boldsymbol{\tau}\cdot\mathbf{y}}. \end{aligned} \tag{9}$$

Here we introduced a new variable $\boldsymbol{\tau}=\tau\hat{k}$ in the last line. Comparing Eq. (9) with scaling property (4), we obtain

$$G_3(\hat{k},\mathbf{y})=\int_0^\infty d\tau\tau\tilde{f}(\boldsymbol{\tau})e^{i2\pi\boldsymbol{\tau}\cdot\mathbf{y}}. \tag{10}$$

The right-hand side (rhs) of Eq. (10) is reminiscent of an inverse Fourier transform for the image function $f(\mathbf{x})$, which is what we want to obtain in our image reconstruction scheme. To make such an intuition more rigorous, we need to increase the power of τ in Eq. (10) from τ to τ^2 so that we have the correct Jacobian factor for a three-dimensional volume element in the spherical coordinate system. This can be easily accomplished by taking a derivative with respect to focal trajectory parameter t in Eq. (10). That is,

$$\frac{1}{2\pi i\hat{k}\cdot\mathbf{y}'(t)}\frac{\partial}{\partial t}G_3[\hat{k},\mathbf{y}(t)]=\int_0^\infty d\tau\tau^2\tilde{f}(\boldsymbol{\tau})e^{i2\pi\boldsymbol{\tau}\cdot\mathbf{y}}. \tag{11}$$

One can now recognize that the rhs of the above equation is nothing but the radial part of an inverse Fourier transform of $\tilde{f}(\boldsymbol{\tau})$. Therefore, we can obtain the image function by integrating over all the possible orientations $\hat{k}$ of the vector $\boldsymbol{\tau}=\tau\hat{k}$. Thus we obtain

$$\begin{aligned} &\int_{S_k^2} d\Omega_k \frac{1}{2\pi i\hat{k}\cdot\mathbf{y}'(t)}\frac{\partial}{\partial t}G_3[\hat{k},\mathbf{y}(t)] \\ &\quad = \int_{S_k^2} d\Omega_k \int_0^\infty d\tau\tau^2\tilde{f}(\boldsymbol{\tau})e^{i2\pi\boldsymbol{\tau}\cdot\mathbf{y}}, \end{aligned} \tag{12}$$

where $d\Omega_k=\sin\theta_k d\theta_k d\phi_k$ is angular integral measure over a sphere with latitude angle θ_k and longitude angle ϕ_k.

The rhs of Eq. (12) is a Fourier inversion for image function $f(\mathbf{x})$ when we impose the following condition,

$$\hat{k}\cdot\mathbf{x}=\hat{k}\cdot\mathbf{y}(t), \tag{13}$$

on the source trajectory $\mathbf{y}(t)$ for each point $\mathbf{x}$ within the ROI and an arbitrary unit vector $\hat{k}$. In other words, with condition (13), we can replace $\boldsymbol{\tau}\cdot\mathbf{y}$ the rhs of Eq. (12) by $\boldsymbol{\tau}\cdot\mathbf{x}$ for all the image points within the ROI so that the rhs of the Eq. (12) is nothing but $f(\mathbf{x})$. Thus we rederived Tuy's cone-beam inversion formula[3]

$$f(\mathbf{x})=\int_{S_k^2} d\Omega_k \frac{1}{2\pi i\hat{k}\cdot\mathbf{y}'(t)}\frac{\partial}{\partial t}G_3[\hat{k},\mathbf{y}(t)]\big|_{\hat{k}\cdot\mathbf{x}=\hat{k}\cdot\mathbf{y}(t)}. \tag{14}$$

This inversion formula also tells us Tuy's data sufficiency conditions for an accurate reconstruction of a ROI from cone-beam projections. These conditions are:

Condition 1: $\hat{k}\cdot\mathbf{x}=\hat{k}\cdot\mathbf{y}(t)$;

Condition 2: $\hat{k}\cdot\mathbf{y}'(t)\neq 0$.

The meaning of the above two mathematical formulas is interpreted and summarized in accordance with Tuy's original data sufficiency condition:[3]

To accurately reconstruct an image for a ROI, all the planes passing through the ROI should intersect the source trajectory at least once in a nontangential and nonended way.

We would like to elaborate more on this data sufficiency condition. First, to define an intermediate function $G_3[\mathbf{k},\mathbf{y}(t)]$ for a specific focal spot $\mathbf{y}(t)$ on the source trajectory, we need to know all the line integrals in a cone containing the whole object. In other words, in the inversion formula (14), the data truncation is not allowed. Second, there is a derivative with respect to source trajectory parameter t. Therefore, we need to extend the source trajectory

slightly further than specified by condition 1 in order to make sense of the derivative at the end points. In the next section, after we rewrite the inversion formula (14) into a form with an integral over the source trajectory parameter t, we are able to transform this derivative to some other functions[16] so that this ''nonended'' restriction could be further relaxed. Third, one may think that the nontangential condition $\hat{k}\cdot\mathbf{y}'(t)\neq 0$ is a hard constraint on the source trajectory. However, as we pointed out in our previous paper,[16] the key observation is that there is an integral over unit vector $\hat{k}$. Therefore, the question about the singularities at $\hat{k}\cdot\mathbf{y}'(t)=0$ is whether we can properly regularize the integral over $\hat{k}$. If we have a proper way to regularize the integral, then the condition $\hat{k}\cdot\mathbf{y}'(t)=0$ should not be a problem in practice. In other words, a proper regularization scheme can be used to relax the Tuy's data sufficiency condition. In the next section, we will show how this integral can be properly regularized by a signum function $\mathrm{sgn}[\hat{k}\cdot\mathbf{y}'(t)]$ [see the discussion after Eq. (27)]. Therefore, we formulate our relaxed data sufficiency condition as follows: *To accurately reconstruct an image for a ROI, all the planes passing through the ROI should intersect source trajectory at least once in a nonended way*.

III. THE DERIVATION OF CONE-BEAM FBP RECONSTRUCTION FORMULA

In the following, we will show how to derive a FBP reconstruction formula from Tuy's formula (14) and show how Tuy's data sufficiency condition can be relaxed. To highlight the similar theoretical structure we extracted in Ref. 16, we separate the discussion into several parts.

A. Symmetry of intermediate function $G_3(\hat{k},\mathbf{y})$

Here, we discuss some symmetry properties of the intermediate function $G_3(\hat{k},\mathbf{y})$. To do so, we choose to work in a spherical coordinate system,

$$G_3(\hat{k},\mathbf{y})=\int d^3\mathbf{r}\,g(\mathbf{r},\mathbf{y})e^{-i2\pi\hat{k}\cdot\mathbf{r}}=\int_{S_r^2}d\Omega_r\int_0^\infty drr^2 g(r\hat{r},\mathbf{y})e^{-i2\pi r\hat{k}\cdot\hat{r}}, \tag{15}$$

where $d\Omega_r=\sin\theta_r d\theta_r d\phi_r$ is the integral measure over a spherical surface S^2 with latitude and longitude angles θ_r, ϕ_r, respectively. Using the scaling property (2), we obtain

$$\begin{aligned}G_3(\hat{k},\mathbf{y})&=\int_{S_r^2}d\Omega_r g(\hat{r},\mathbf{y})\int_0^\infty drre^{-i2\pi r\hat{k}\cdot\hat{r}}\\&=\frac{1}{2}\int_{S_r^2}d\Omega_r g(\hat{r},\mathbf{y})\int_{-\infty}^{+\infty}dr(r+|r|)e^{-i2\pi r\hat{k}\cdot\hat{r}}\\&=G_3^{\mathrm{even}}(\hat{k},\mathbf{y})+G_3^{\mathrm{odd}}(\hat{k},\mathbf{y}).\end{aligned} \tag{16}$$

Here we decomposed the intermediate function $G_3(\hat{k},\mathbf{y})$ into an even part and odd part under the reflection transformation: $\hat{k}\rightarrow-\hat{k}$,

$$\begin{aligned}G_3^{\mathrm{odd}}(\hat{k},\mathbf{y})&=\frac{1}{2}\int_{S_r^2}d\Omega_r g(\hat{r},\mathbf{y})\int_{-\infty}^{+\infty}drre^{-i2\pi r\hat{k}\cdot\hat{r}}\\&=-\frac{1}{4\pi i}\int_{S_r^2}d\Omega_r g(\hat{r},\mathbf{y})\delta'(\hat{k}\cdot\hat{r}).\end{aligned} \tag{17}$$

$$\begin{aligned}G_3^{\mathrm{even}}(\hat{k},\mathbf{y})&=\frac{1}{2}\int_{S_r^2}d\Omega_r g(\hat{r},\mathbf{y})\int_{-\infty}^{+\infty}dr|r|e^{-i2\pi r\hat{k}\cdot\hat{r}}\\&=\frac{1}{2}\int_{S_r^2}d\Omega_r g(\hat{r},\mathbf{y})h_R(\hat{k}\cdot\hat{r}),\end{aligned} \tag{18}$$

where $h_R(\hat{k}\cdot\hat{r})$ is the standard one-dimensional ramp filter. It is easy to show the following symmetries:

$$G_3^{\mathrm{odd}}(-\mathbf{k},\mathbf{y})=-G_3^{\mathrm{odd}}(\mathbf{k},\mathbf{y}),\quad G_3^{\mathrm{even}}(-\mathbf{k},\mathbf{y})=G_3^{\mathrm{even}}(\mathbf{k},\mathbf{y}). \tag{19}$$

Such a decomposition also substantiates our intuitive arguments given in the preceding section. Namely, we represent $G_3[\hat{k},\mathbf{y}(t)]$ by two fundamental homogeneous functions $\delta'(x)$ and $h_R(x)$. In the context of cone-beam reconstruction, such a decomposition was first used in Ref. 7. If we take into account the fact that the factor $\hat{k}\cdot\mathbf{y}'(t)$ in the inversion formula (14) is also odd under the above reflection transformation: $\hat{k}\rightarrow-\hat{k}$, we conclude that only the derivative filter term $G_3^{\mathrm{odd}}(\hat{k},\mathbf{y})$ contributes in the Tuy's inversion formula while the contribution of the ramp filter term $G_3^{\mathrm{even}}(\hat{k},\mathbf{y})$ vanishes after we perform the integral over unit vector $\hat{k}$ in Eq. (14). An alternative argument for this conclusion is the following: The odd term $G_3^{\mathrm{odd}}(\hat{k},\mathbf{y})$ is purely imaginary and the even term $G_3^{\mathrm{even}}(\hat{k},\mathbf{y})$ is purely real. Therefore, the reality condition of the image function $f(\mathbf{x})$ in Eq. (14) enforces the contribution of the even part to be zero. Thus we have

$$f(\mathbf{x})=\int_{S_k^2}d\Omega_k\frac{1}{2\pi i\hat{k}\cdot\mathbf{y}'(t)}\frac{\partial}{\partial t}G_3^{\mathrm{odd}}[\hat{k},\mathbf{y}(t)]\big|_{\hat{k}\cdot\mathbf{x}=\hat{k}\cdot\mathbf{y}(t)}. \tag{20}$$

Since there is a derivative of delta function in $G_3^{\mathrm{odd}}[\hat{k},\mathbf{y}(t)]$, it is more convenient to remove the derivative of a delta function via integration by parts. This step leads to

$$\begin{aligned}G_3^{\mathrm{odd}}(\hat{k},\mathbf{y})&=\frac{i}{4\pi}\int_{S_r^2}d\Omega_r g(\hat{r},\mathbf{y})\delta'(\hat{k}\cdot\hat{r})\\&=-\frac{i}{4\pi}\int_{S_r^2}d\Omega_r\hat{k}\cdot\nabla_{\hat{r}}g(\hat{r},\mathbf{y})\delta(\hat{k}\cdot\hat{r}).\end{aligned} \tag{21}$$

The meaning of $\hat{k}\cdot\nabla_{\hat{r}}g(\hat{r},\mathbf{y})$ is the directional derivative along the direction $\hat{k}$ of cone-beam data $g(\hat{r},\mathbf{y})$ with respect to unit vector $\hat{r}$. In other words, it is the projection of the gradient of function $g(\hat{r},\mathbf{y})$ onto the direction $\hat{k}$.

B. Weighting function for the redundant data

As a matter of fact, there might be several focal points $\mathbf{y}(t_j)$, $j=1,2,\ldots$ to satisfy Eq. (13) for a specific point $\mathbf{x}$ of the ROI and a unit vector $\hat{k}$. Therefore, a weighting scheme is necessary to handle these possible solutions. In Tuy's original inversion formula (14), a special weighting scheme has been assumed: using one of these solutions and discarding all others. Theoretically, this scheme does not cause any problem. However, such a weighting scheme may not be the optimal solution in practice. First, the acquired data are noisy in reality. From the experience of the fan-beam reconstruction, it is well known that different weighting schemes may have different noise level in a reconstructed image.[18,19] Second, and even more important, a proper choice of the weighting function may provide a way to solve the long object problem.[15] The question of how to optimize the weighting function is an important topic but it is beyond the scope of the present paper. In this paper, we keep the functional form of weighting function as general as possible. Since the solutions of Eq. (13) strongly depend on the image point $\mathbf{x}$ within a ROI and the unit vector $\hat{k}$, the maximally possible form of the weighting function allowed by the current framework is $w(\mathbf{x},\hat{k};t_j)$ $[j=1,2,\ldots,n(\mathbf{x},\hat{k})]$, where $n(\mathbf{x},\hat{k})$ is the total number of solutions of Eq. (13) at a specific point $\mathbf{x}$ and specific unit vector $\hat{k}$. The weighting function should also be constrained by the following normalization condition:

$$\sum_{j=1}^{n(\mathbf{x},\hat{k})} w(\mathbf{x},\hat{k};t_j)=1. \tag{22}$$

If the number of solution $n(\mathbf{x},\hat{k})$ becomes infinite, the above-presented summation should be understood as an integral over source parameter t.

After we weight the redundant data by the weighting function $w(\mathbf{x},\hat{k};t_j)$, Eq. (20) can be further modified into the following form:

$$f(\mathbf{x})=\int_{S_k^2} d\Omega_k \sum_{j=1}^{n(\mathbf{x},\hat{k})} \frac{w(\mathbf{x},\hat{k};t_j)}{2\pi i\hat{k}\cdot\mathbf{y}'(t_j)} \frac{\partial}{\partial q} G_3^{\mathrm{odd}}[\hat{k},\mathbf{y}(q)]|_{q=t_j}. \tag{23}$$

Compared with Eq. (14), Eq. (23) amounts to taking the average over contributions from all the focal points that satisfy Eq. (13), not simply taking one and discarding others as implied in Eq. (14).

C. From summation to integral along the source trajectory

Modifications from Tuy's original inversion (14) to Eq. (23) with $G_3^{\mathrm{odd}}(\hat{k},\mathbf{y})$ in Eq. (21) have been important progress. However, even using the simple equal weighting scheme, the numerical implementation of formula (23) is still complicated.[7] Note that Eq. (23) dictates that we need to numerically handle four integrals (two over $\hat{k}$ and two over $\hat{r}$), a summation over multiple-solutions, and a derivative along the source trajectory. However, as we have shown in the fan-beam case,[16] the following property[20,21] of delta functions can be used to change the discrete summation into an integral along the source trajectory. That is:

$$\int_{-\infty}^{+\infty} dt\, f(t)\,\delta[g(t)]=\sum_i \frac{f(t_i)}{|g'(t_i)|}, \quad g'(t_i)\neq 0. \tag{24}$$

where t_i $(i=1,2,\ldots)$ are the roots of equation $g(t)=0$. After we set functions $f(t)$ and $g(t)$ as

$$f(t)=\mathrm{sgn}[\hat{k}\cdot\mathbf{y}'(t)]w(\mathbf{x},\hat{k};t)\frac{\partial}{\partial q}G_3^{\mathrm{odd}}(\hat{k},\mathbf{y}(q))|_{q=t}, \tag{25}$$

$$g(t)=\hat{k}\cdot[\mathbf{x}-\mathbf{y}(t)], \tag{26}$$

using Eq. (24), the summation in Eq. (23) can be written into an integral over the parameter t of the source trajectory, i.e.,

$$\begin{aligned} f(\mathbf{x}) &= \frac{1}{2\pi i}\int_{S_k^2} d\Omega_k \int dt\, w(\mathbf{x},\hat{k};t)\,\mathrm{sgn}[\hat{k}\cdot\mathbf{y}'(t)] \\ &\quad\times\frac{\partial}{\partial q}G_3^{\mathrm{odd}}[\hat{k},\mathbf{y}(q)]|_{q=t}\delta[\hat{k}\cdot(\mathbf{x}-\mathbf{y}(t))] \\ &= \frac{1}{2\pi i}\int dt\int_{S_k^2} d\Omega_k \frac{w(\mathbf{x},\hat{k};t)}{|\mathbf{x}-\mathbf{y}(t)|}\mathrm{sgn}[\hat{k}\cdot\mathbf{y}'(t)]\frac{\partial}{\partial q} \\ &\quad\times G_3^{\mathrm{odd}}[\hat{k},\mathbf{y}(q)]|_{q=t}\delta[\hat{k}\cdot\hat{\beta}]. \end{aligned} \tag{27}$$

Here we introduced a unit vector $\hat{\beta}$,

$$\hat{\beta}=\frac{\mathbf{x}-\mathbf{y}(t)}{|\mathbf{x}-\mathbf{y}(t)|}. \tag{28}$$

From the first line to the second line in Eq. (27), we used the scaling property of Dirac delta function $\delta(ax)=\delta(x)/|a|$ with a substitution of $a=|\mathbf{x}-\mathbf{y}(t)|$ and $x=\hat{k}\cdot\hat{\beta}$.

In Tuy's original inversion formula (14), a "nontangential" condition on the source trajectory[3] was imposed to avoid zero denominator when $\hat{k}\cdot\mathbf{y}'(t)=0$ is satisfied. Consequently, in Eq. (27), the values of the factor $\mathrm{sgn}[\hat{k}\cdot\mathbf{y}'(t)]$ are ± 1. From Eq. (14) to Eq. (27), two modifications have been introduced: First, a general weighting scheme is used. Second, the intermediate function has been separated into even- (real) and odd (imaginary) parts. However, the data sufficiency conditions are still the same as Tuy's original one.

Equation (27) provides us the ability to regularize the sigularities from the tangential condition: $\hat{k}\cdot\mathbf{y}'(t)=0$. The key observation is that the conventional definition of the signum function $\mathrm{sgn}(x)$ takes the value zero at $x=0$. Therefore, by adding the value zero back to signum function in Eq. (27), when the above tangential condition is satisfied, Eq. (27) can be viewed as a regularized version of the original Tuy's formula Eq. (14). The acceptance of this modified formula allows us to relax Tuy's data sufficiency condition to include $\hat{k}\cdot\mathbf{y}'(t)=0$. The definition of the function $\mathrm{sgn}(x)$ automatically enforces it to take value zero at $\hat{k}\cdot\mathbf{y}'(t)=0$. *Therefore, we can relax the "nontangential" restriction on the source trajectory as we stated at the end of Sec.* II.

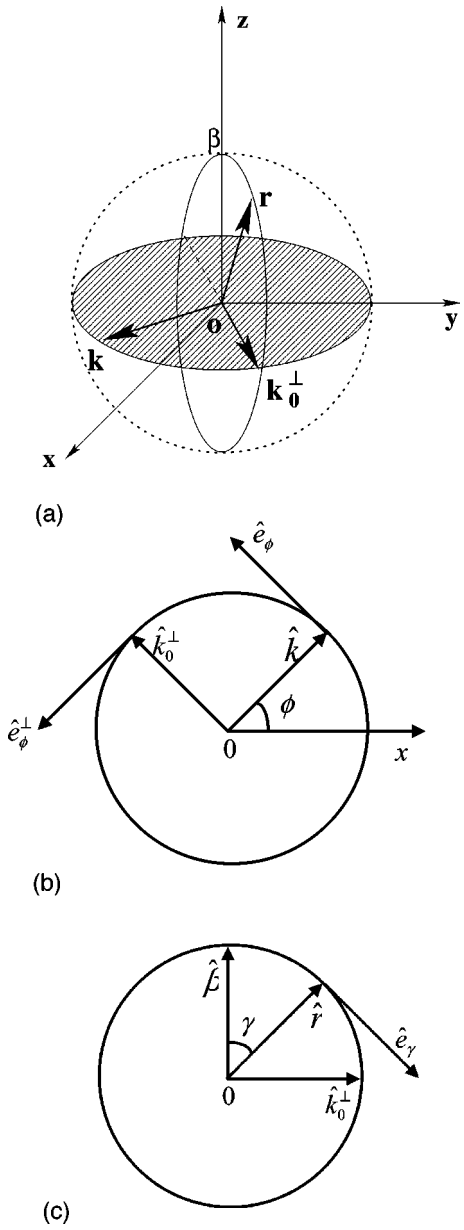

FIG. 2. (a) The coordinate system and the possible values for unit vectors $\hat{k}$ and $\hat{r}$. Unit vector $\hat{\beta}$ is aligned along the z axis. Unit vectors $\hat{k}$ and $\hat{k}_0^{\perp}$ lie in the horizontal plane (shaded); unit vectors $\hat{\beta}$, $\hat{r}$, and $\hat{k}_0^{\perp}$ lie in the vertical plane. (b) Unit vectors $\hat{k}$, $\hat{k}_0^{\perp}$ and the corresponding tangential vectors $\hat{e}_{\phi}$ and $\hat{e}_{\phi}^{\perp}$. (c) Tangential vector $\hat{e}_{\gamma}$ for the unit vector $\hat{r}$.

D. Simplification of integrals over unit vectors $\hat{k}$ and $\hat{r}$

After substituting Eq. (21) into Eq. (27), we obtain:

$$f(\mathbf{x}) = -\frac{1}{8\pi^2}\int dt \int_{S_k^2} d\Omega_k \int_{S_r^2} d\Omega_r \delta(\hat{k}\cdot\hat{\beta}) \times \delta(\hat{k}\cdot\hat{r})\mathcal{P}(\hat{k},\hat{\beta},\hat{r},t;\mathbf{x}), \tag{29}$$

where $\mathcal{P}(\hat{k},\hat{\beta},\hat{r},t;\mathbf{x})$ is a short-hand symbol for

$$\mathcal{P}(\hat{k},\hat{\beta},\hat{r},t;\mathbf{x}) = \frac{w(\mathbf{x},\hat{k};t)}{|\mathbf{x}-\mathbf{y}(t)|}\operatorname{sgn}[\hat{k}\cdot\mathbf{y}'(t)](\hat{k}\cdot\nabla_{\hat{r}}) \times\left(\frac{\partial g[\hat{r},\mathbf{y}(t)]}{\partial t}\right). \tag{30}$$

In Eq. (29), a symbol $\mathcal{P}$ is introduced to highlight the structure of the two Dirac delta functions. Since $\hat{k}$ and $\hat{r}$ are integral variables, we have some freedom to choose a convenient coordinate system in the computation. The structure of the double delta functions suggests such a convenient system: the unit vector $\hat{\beta}$ is aligned along the z direction, see Fig. 2(a). In other words, the unit vector $\hat{\beta}$ has coordinates

$$\hat{\beta} = (0,0,1). \tag{31}$$

We can parametrize the variables $\hat{k}$ and $\hat{r}$ in this local coordinate system. The delta function $\delta(\hat{k}\cdot\hat{\beta})$ dictates that the integral over unit vector $\hat{k}$ will single out those vectors moving along a great circle in the xy plane; namely, the plane perpendicular to $\hat{\beta}$. Therefore, we can parametrize $\hat{k}$ in the chosen local coordinate system as

$$\hat{k}(\phi) = (\cos\phi, \sin\phi, 0), \quad \phi\in[0,2\pi). \tag{32}$$

In other words, the delta function $\delta(\hat{k}\cdot\hat{\beta})$ reduces the integral over a unit sphere into a single integral over angular variable ϕ, $\phi\in[0,2\pi)$.

To figure out a parametrization of vector $\hat{r}$, we define a unit vector $\hat{k}_0^{\perp}$, which is perpendicular to $\hat{k}$ and lies in the xy plane [see Fig. 2(b)]. In terms of variable ϕ, the unit vector $\hat{k}_0^{\perp}$ can be written as

$$\hat{k}_0^{\perp}(\phi) = (-\sin\phi, \cos\phi, 0), \quad \phi\in[0,2\pi). \tag{33}$$

Obviously, the three unit vectors $\hat{\beta}$, $\hat{k}$, $\hat{k}_0^{\perp}$ are mutually perpendicular. The delta function $\delta(\hat{k}\cdot\hat{r})$ implies that we can reduce the integral over a unit sphere $\hat{r}$ into a single integral over a great circle which is perpendicular to the vector $\hat{k}$. Using the unit vectors $\hat{\beta}$ and $\hat{k}_0^{\perp}$, the vector $\hat{r}$ can be parametrized by a rotation parameter γ as

$$\hat{r} = \hat{\beta}\cos\gamma + \hat{k}_0^{\perp}(\phi)\sin\gamma, \quad \gamma\in[0,2\pi) = (-\sin\gamma\sin\phi, \sin\gamma\cos\phi, \cos\gamma). \tag{34}$$

The angle γ is measured from the z direction. The geometrical relations of the above decomposition are shown in Fig. 2(c).

Using the above-given parametrization, we can change the two integrals over the unit spheres $S_{\hat{k}}^2$ and $S_{\hat{r}}^2$ into two single integrals over parameters ϕ and γ, respectively. That is,

$$f(\mathbf{x}) = -\frac{1}{8\pi^2}\int dt \frac{1}{|\mathbf{x}-\mathbf{y}(t)|} \times \int_0^{2\pi} d\phi \,\mathrm{sgn}[\hat{k}(\phi)\cdot\mathbf{y}'(t)] w[\hat{k}(\phi),\mathbf{x};t] \times \int_0^{2\pi} d\gamma (\hat{k}\cdot\nabla_{\hat{r}}) \left(\frac{\partial}{\partial t} g[\hat{r}(\gamma,\phi),\mathbf{y}(t)] \right). \quad (35)$$

As shown in the Appendix, we can explicitly express the gradient operator in terms of variables ϕ and γ, namely

$$\nabla_{\hat{r}} = \hat{e}_{\phi}^{\perp} \frac{1}{\sin\gamma} \frac{\partial}{\partial\phi} + \hat{e}_{\gamma} \frac{\partial}{\partial\gamma}, \quad (36)$$

where the unit vector $\hat{e}_{\phi}^{\perp}$ and $\hat{e}_{\gamma}$ are shown in Figs. 2(b) and 2(c), respectively. Since $\hat{k}$, $\hat{\beta}$, and $\hat{k}_0^{\perp}$ are mutually perpendicular [see Fig. 2(a)], we obtain

$$\hat{k}\cdot\hat{e}_{\phi}^{\perp} \equiv -1, \quad \hat{k}\cdot\hat{e}_{\gamma} \equiv 0. \quad (37)$$

These two results are also indicated in Figs. 2(b) and 2(c). Combining Eq. (36) with Eq. (37),

$$\hat{k}\cdot\nabla_{\hat{r}} = -\frac{1}{\sin\gamma}\frac{\partial}{\partial\phi}. \quad (38)$$

Substituting Eq. (38) into Eq. (35), we obtain

$$f(\mathbf{x}) = \frac{1}{8\pi^2}\int dt \frac{1}{|\mathbf{x}-\mathbf{y}(t)|} \int_0^{2\pi} d\phi \,\mathrm{sgn}[\hat{k}(\phi)\cdot\mathbf{y}'(t)] \times w[\hat{k}(\phi),\mathbf{x};t] \times \int_0^{2\pi} \frac{d\gamma}{\sin\gamma} \left(\frac{\partial^2}{\partial\phi\partial t} g[\hat{r}(\gamma,\phi),\mathbf{y}(t)] \right)$$

$$= \frac{1}{8\pi^2}\int dt \frac{1}{|\mathbf{x}-\mathbf{y}(t)|} \int_0^{2\pi} \frac{d\gamma}{\sin\gamma} \times \int_0^{2\pi} d\phi \,\mathrm{sgn}[\hat{k}(\phi)\cdot\mathbf{y}'(t)] w[\hat{k}(\phi),\mathbf{x};t] \times \frac{\partial}{\partial\phi}\left(\frac{\partial}{\partial q} g[\hat{r}(\gamma,\phi),\mathbf{y}(q)]\big|_{q=t} \right). \quad (39)$$

In this way, we managed to reduce the integrals over unit vectors $\hat{k}$ and $\hat{r}$ into two single integrals over angular variables ϕ and γ, respectively.

E. Additional constraint on the weighting functions

In Sec. III D, we managed to obtain a reconstruction formula (39) by three integrals over the parameters t, ϕ, and γ. These parameters were used to define the projections $g[\hat{r}(\phi,\gamma),\mathbf{y}(t)]$. In the following, we demonstrate that a further constraint on the weighting function allows for an even simpler reconstruction formula. To do so, we perform integration by parts for the integration over ϕ in Eq. (39). We thus obtain

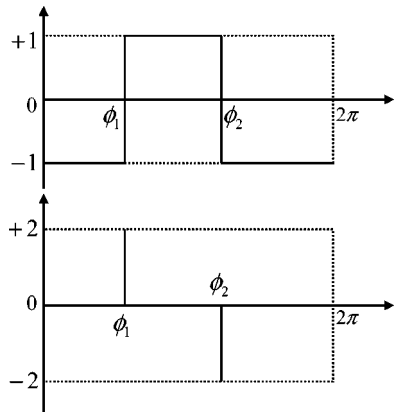

FIG. 3. The schematic representation of sign function $\mathrm{sgn}[\hat{k}\cdot\mathbf{y}'(t)]$ and its derivative with respect to ϕ.

$$f(\mathbf{x}) = -\frac{1}{8\pi^2}\int dt \frac{1}{|\mathbf{x}-\mathbf{y}(t)|} \int_0^{2\pi} \frac{d\gamma}{\sin\gamma} \int_0^{2\pi} d\phi \times \frac{\partial}{\partial\phi}(\mathrm{sgn}[\hat{k}(\phi)\cdot\mathbf{y}'(t)] w[\mathbf{x},\hat{k}(\phi);t]) \times \frac{\partial}{\partial q} g[\hat{r}(\gamma,\phi),\mathbf{y}(q)]\big|_{q=t}. \quad (40)$$

Here we used the fact that the boundary term vanishes since the integral over variable ϕ is in the interval $[0,2\pi)$. At first glance, it appears that integration by parts may not provide further insight. However, a simplification may occur if we take a close look at the derivative

$$\frac{\partial}{\partial\phi}(\mathrm{sgn}[\hat{k}(\phi)\cdot\mathbf{y}'(t)] w[\mathbf{x},\hat{k}(\phi);t]) = w[\mathbf{x},\hat{k}(\phi);t] \frac{\partial}{\partial\phi}\mathrm{sgn}[\hat{k}(\phi)\cdot\mathbf{y}'(t)] + \mathrm{sgn}[\hat{k}(\phi)\cdot\mathbf{y}'(t)] \frac{\partial}{\partial\phi} w[\mathbf{x},\hat{k}(\phi);t]. \quad (41)$$

The first term involves a derivative of $\mathrm{sgn}(x) = 2u(x) - 1$ where $u(x)$ is a step function. Consequently, this derivative generates the Dirac delta function $2\delta(x)$. After performing the integration over ϕ, the integral is reduced to a summation over the discontinuous points of the function $\mathrm{sgn}(x)$. We label the zeros of the function $\mathrm{sgn}[\hat{k}(\phi)\cdot\mathbf{y}'(t)]$ as ϕ_m. Note that ϕ_m satisfies

$$\hat{k}(\phi_m)\cdot\mathbf{y}'(t) = 0. \quad (42)$$

Noting that the unit vector $\hat{\beta}$ is also perpendicular to the vector $\hat{k}$, the combination of this fact with Eq. (42) dictates that the unit vector $\hat{k}$ is perpendicular to a plane spanned by the two vectors $\hat{\beta}$ and $\mathbf{y}'(t)$. Thus, we have two possible orientations for unit vector $\hat{k}(\phi_m)$. In other words, there are two solutions for Eq. (42).

We schematically draw the function $\mathrm{sgn}[\hat{k}(\phi)\cdot\mathbf{y}'(t)]$ vs variable ϕ in Fig. 3. Since each discontinuous point ϕ_m cor-

responds to a Dirac delta function after taking the derivative, we obtain

$$\frac{\partial}{\partial \phi}\mathrm{sgn}[\hat{k}(\phi)\cdot\mathbf{y}'(t)]=\sum_m A_m\delta(\phi-\phi_m), \tag{43}$$

where $A_m=\pm 2$ is the impulse intensity. If the discontinuous point is a kink ($_-|^-$), the sign is positive; for an anti-kink ($^-|_-$), the sign is negative (see Fig. 3).

On the other hand, the contribution of the second term in Eq. (41) is generally nonzero. Up until this point, the choice of the weighting function $w[\mathbf{x},\hat{k}(\phi);t]$ is completely arbitrary provided it satisfies the normalization condition (22). Therefore, *we can choose an appropriate weighting function* $w[\mathbf{x},\hat{k}(\phi);t]$ *to make this term locally vanish*. In other words, we can impose the following constraint on the choice of weighting functions:

$$\frac{\partial}{\partial \phi}w[\mathbf{x},\hat{k}(\phi);t]=0 \tag{44}$$

in order to make the second term in Eq. (41) vanish locally. We would like to emphasize that condition (44) does not imply a globally ϕ-independent weighting function. Equation (44) may be further clarified by considering the following physical scenario: For a single image point $\mathbf{x}$ and a source point labeled by parameter t, we draw a straight line between these two points. The normal vectors to those planes containing this straight line will move on a unit circle. The number of intersection points between these planes and the source trajectory may vary upon moving the unit vector $\hat{k}$ along the above unit circle. Equation (44) implies that the weighting function should be locally constant between two different intersection numbers. As a consequence, over the range of $\phi\in[0,2\pi)$ the second term in Eq. (41) is reduced into a summation of several Dirac-delta functions at discontinuous points of weighting function. That is:

$$\mathrm{sgn}[\hat{k}(\phi)\cdot\mathbf{y}'(t)]\frac{\partial}{\partial \phi}w[\mathbf{x},\hat{k}(\phi);t]$$

$$=\sum_n B_n\,\mathrm{sgn}[\hat{k}(\phi_n)\cdot\mathbf{y}'(t)]\delta(\phi-\phi_n). \tag{45}$$

Therefore, after we combine Eq. (43) with Eq. (45), Eq. (41) is changed into a summation of weighted Dirac-delta functions. In other words, we obtain

$$\frac{\partial}{\partial \phi}(\mathrm{sgn}[\hat{k}(\phi)\cdot\mathbf{y}'(t)]w[\mathbf{x},\hat{k}(\phi);t])$$

$$=\sum_l C_l(\mathbf{x},t)\,\delta(\phi-\phi_l), \tag{46}$$

where the index l runs over all the possible values of indices m and n in Eqs. (43) and (45), respectively. An integral over the range of $[\phi_l-\varepsilon,\phi_l+\varepsilon]$ with ε the positive infinitesimal yields the coeefficient $C_l(\mathbf{x},t)$:

$$C_l(\mathbf{x},t)=\int_{\phi_l-\varepsilon}^{\phi_l+\varepsilon}d\phi\frac{\partial}{\partial \phi}(\mathrm{sgn}[\hat{k}(\phi)\cdot\mathbf{y}'(t)]w[\mathbf{x},\hat{k}(\phi);t])$$

$$=\mathrm{sgn}[\hat{k}(\phi)\cdot\mathbf{y}'(t)]w[\mathbf{x},\hat{k}(\phi);t]\big|_{\phi=\phi_m-\varepsilon}^{\phi=\phi_m+\varepsilon}. \tag{47}$$

The values of factor $C_l(\mathbf{x},t)$ are determined by the definition of the weighting function and signum function near the discontinuous points ϕ_l's. The result of Eq. (46) is independent of the specific geometrical shape of the image object. Rather, it is determined by the scanning geometry. Thus we termed it a *structure factor* of the scanning geometry.

F. Cone-beam FBP reconstruction formula

In the following, we assume that a normalized weighting function has been chosen to satisfy Eq. (46). After substituting Eqs. (46) and (47) into Eq. (40), we obtain

$$f(\mathbf{x})=-\frac{1}{8\pi^2}\sum_l\int dt\frac{C_l(\mathbf{x},t)}{|\mathbf{x}-\mathbf{y}(t)|}\int_0^{2\pi}\frac{d\gamma}{\sin\gamma}\frac{\partial}{\partial q}g$$

$$\times[\hat{k}_0^{\perp}(\phi_l)\sin\gamma+\hat{\beta}\cos\gamma,\mathbf{y}(q)]\big|_{q=t}, \tag{48}$$

where the structure factor $C_l(\mathbf{x},t)$ is given by Eq. (47) and normalized weighting function $w(\mathbf{x},\hat{k};t)$ satisfies Eq. (46). This reconstruction formula is the one discovered by Katsevich recently.[15]

Several remarks on Eq. (48) are in order. First, the number of terms in the summation is dependent on the discontinuiuty of the weighting function. Second, each term in the summation is a twofold integral. These two features are very important in the improvement of the computational efficiency in the cone-beam image reconstruction. Third, only the projections at $\phi=\phi_l$ are required. In other words, only a fan region of the data in the cone-beam projections [labeled by the unit vector $\hat{r}(\gamma,\phi)$] is used. This feature implies that data truncation is allowed. Thus, this feature provides the basis for a new way to solve the so-called long object problem.[13,15] Fourth, followed from the derivation of Eq. (48), the constraints on the weighting function (46) and (22) are *necessary conditions* for the final result (48). Finally, the cone-beam reconstruction formula (48) has the obvious FBP structure, though the shift-invariant property is not explicit yet. However, as shown by Katsevich,[13,15] it can be proved to be shift-invariant for a specific scanning geometry.

IV. CONCLUSIONS AND DISCUSSIONS

In this paper, a derivation of Katsevich's FBP cone-beam image reconstruction formula (48) is presented in the same fashion as that in Ref. 16 where the FBP fan-beam reconstruction algorithms were derived. The derivation procceded according to the following steps: We start with Tuy's inversion scheme, utilize the hidden symmetries in the intermediate function, appropriately handle the data redundancy, change the weighted average (summation) into an integral along the source trajectory, and finally impose an additional constraint on the weighting function. These steps directly lead us to the desired reconstruction formula (48). These major steps in the derivation are equivalent to those used in

the fan-beam case.[16] Compared with the fan-beam case, the only dimensional difference is that an additional constraint [Eq. (46)] has to be imposed on the weighting functions in order to derive the final FBP reconstruction formula (48). In contrast, a mathematically exact FBP reconstruction formula exists for an arbitrarily chosen normalized weighting function in the fan-beam case.

Compared with Tuy's original work,[3] the nontangential condition in his original data sufficiency condition is relaxed. This relaxation is a consequence of the "sgn-regulator" ($\mathrm{sgn}[\hat{k}\cdot\mathbf{y}'(t)]$) used in the derivation in order to rewrite the weighted summation over the redundant data into an integral along the source trajectory. Furthermore, in Tuy's original formula, data truncation is not allowed. However, after the introduction of the additional constraint on the weighting function, only those projections at $\phi=\phi_l$ appeared in the reconstruction formula. Thus, the final reconstruction formula (48) *does* allow data truncation in the ϕ direction. This improvement is due to the step discussed in Sec. III C, where the integral along the source trajectory was introduced by the properties of a delta function. Otherwise it would be difficult to eliminate the Tuy's intermediate function $G_3[\hat{k},\mathbf{y}(t)]$.

In summary, this work in combination with fan-beam reconstruction[16] establishes a framework to develop image reconstruction algorithms from divergent beam projections. In this way the fan-beam and cone-beam cases may be treated with one unified framework. In this framework, the concepts of Radon space, the Radon transform, and the inverse Radon transform are not necessary. Since we are in the time of transition from single slice and mutislices CT to the true cone-beam CT, we believe that it is important and useful to establish a strong link between fan-beam reconstruction and cone-beam reconstruction methods. This link may allow CT researchers who are familiar with fan-beam CT technologies to smoothly adjust themselves to cone-beam CT.

ACKNOWLEDGMENTS

The author is very grateful for the support and encouragement from Professor Charles A. Mistretta. Special thanks goes to Dr. Sarah K. Patch for bringing Katsevich's works to the author's attention. Thanks also goes to Dr. Alexander Katsevich for stimulating discussions on the present work during 2003 fully 3D meeting at Sait Malo, France. We also acknowledge useful comments and suggestions made by Dr. C. A. Mistretta, Dr. J. Hsieh, Dr. S. K. Patch, Dr. G. L. Zeng, Dr. R. Boutchko, and Dr. X. Tang which prompted the revision of the paper. Finally, we thank GE Medical Systems for funding through a collaboration agreement with the University of Wisconsin.

APPENDIX

In this appendix, we derive Eq. (36) for the gradient operator ∇ in terms of variables γ and ϕ. Using Eq. (34), we can write down the Cartesian representation of unit vector $\hat{r}$,

$$x=-\sin\gamma\sin\phi, \tag{A1}$$

$$y=\sin\gamma\cos\phi, \tag{A2}$$

$$z=\cos\gamma. \tag{A3}$$

Thus, one can calculate the metric g_{ij} as follows:[20]

$$g_{ij}=\frac{\partial x}{\partial q_i}\frac{\partial x}{\partial q_j}+\frac{\partial y}{\partial q_i}\frac{\partial y}{\partial q_j}+\frac{\partial z}{\partial q_i}\frac{\partial z}{\partial q_j}, \tag{A4}$$

where $q_i=\gamma,\phi$. Therefore we obtain

$$g_{\gamma\gamma}=1,\quad g_{\phi\phi}=\sin^2\gamma,\quad g_{\gamma\phi}=g_{\phi\gamma}=0. \tag{A5}$$

Using the above metric, we can write the square of distance element as

$$ds^2=\sum_{ij} g_{ij}dq_i dq_j=(d\gamma)^2+(\sin\gamma d\phi)^2. \tag{A6}$$

Therefore, the gradient operator $\nabla_{\hat{r}}$ is written as[20]

$$\nabla_{\hat{r}}=\hat{e}_\gamma\frac{\partial}{\partial\gamma}+\hat{e}_\phi^{\perp}\frac{1}{\sin\gamma}\frac{\partial}{\partial\phi}, \tag{A7}$$

where $\hat{e}_\gamma$ and $\hat{e}_\phi$ are the tangential unit vectors at point $\hat{r}$. Thus we have derived Eq. (36).

[a]Electronic mail: ghchen@mr.radiology.wisc.edu

[1] L. A. Feldkamp, L. C. Davis, and J. W. Kress, "Practical cone beam algorithm," J. Opt. Soc. Am. A **1**, 612–619 (1984).
[2] G. Wang, T. H. Lin, P. Cheng, and D. M. Shinozaki, "A general cone-beam reconstruction algorithm," IEEE Trans. Med. Imaging **12**, 486–496 (1993).
[3] H. K. Tuy, "An inverse formula for cone-beam reconstruction," SIAM (Soc. Ind. Appl. Math.) J. Appl. Math. **43**, 546–552 (1983).
[4] B. D. Smith, "Image reconstruction from cone-beam projections: Necessary and sufficient conditions and reconstruction methods," IEEE Trans. Med. Imaging **MI-4**, 14–25 (1985).
[5] R. Clack and M. Defrise, "Overview of reconstruction algorithms for exact cone-beam tomography," Proc. SPIE **2299**, 230–241 (1994).
[6] G. L. Zeng and G. T. Gullberg, "A cone-beam tomography algorithm for orthogonal circle-and-line orbit," Phys. Med. Biol. **37**, 563–577 (1992).
[7] G. L. Zeng, R. Clark, and G. T. Gullberg, "Implementation of Tuy's inversion formula," Phys. Med. Biol. **39**, 493–507 (1994).
[8] P. Grangeat, "Mathematical framework of cone beam 3D reconstruction via the first derivative of the Radon transform," in *Mathematical Methods in Tomography*, Lecture Notes in Mathematics, Vol. 1497, edited by G. Herman, A. K. Luis, and F. Natterer (Springer, New York, 1991), pp. 66–97.
[9] M. Defrise and R. Clack, "A cone-beam reconstruction algorithm using shift-variant filtering and cone-beam backprojection," IEEE Trans. Med. Imaging **13**, 186–195 (1994).
[10] H. Kudo and T. Saito, "Derivation and implementation of a cone-beam reconstruction algorithm for non-planar orbit," IEEE Trans. Med. Imaging **13**, 196–211 (1994).
[11] C. Axelsson and P. E. Danielsson, "Three-dimensional reconstruction from cone-beam data in $O(N^3\log N)$ time," Phys. Med. Biol. **39**, 477–491 (1994).
[12] G. Wang, S. Zhao, and P.-C. Cheng, "Exact and Approximate Cone-beam X-ray Microtomography," in *Modern Miscroscopies (I)—Instrumentation and Image Processing* (World Scientific, Singapore, 1998).
[13] A. Katsevich, "Theoretically exact filtered backprojection-type inversion algorithm for Spiral CT," SIAM (Soc. Ind. Appl. Math.) J. Appl. Math. **62**, 2012–2026 (2002).
[14] A. Katsevich, "Analysis of an exact inversion algorithm for spiral cone-beam CT," Phys. Med. Biol. **47**, 2583–2597 (2002).
[15] A. Katsevich, "A general scheme for constructing inversion algorithm for cone beam CT," Int. J. Math. Math. Sci. **21**, 1305–1321 (2003).
[16] G. H. Chen, "A new framework of image reconstruction from fan beam projections," Med. Phys. **30**, 1151–1161 (2003).
[17] F. Natterer, *The Mathematics of Computerized Tomography* (SIAM, Philadelphia, 2001).

[18] G. Wang and M. W. Vannier, ''Helical CT image noise-analytical results,'' Med. Phys. **20**, 1635–1640 (1993).
[19] X. Pan and L. Yu, ''Image reconstruction with shift-variant filtration and its implication for noise and resolution properties in fan-beam tomography,'' Med. Phys. **30**, 590–600 (2003).
[20] G. B. Arfken and H. J. Weber, *Mathematical Methods for Physicists*, 4th ed. (Academic, San Diego, 1995).
[21] R. N. Bracewell, *The Fourier Transform and its Applications*, 2nd ed. (McGraw–Hill, New York, 1986).